Dynamic Covalent Approach to [2]- and [3]Rotaxanes by Utilizing a Reversible Thiol–Disulfide Interchange Reaction

Yoshio Furusho, Tomoya Oku, Toshihide Hasegawa, Akiyoshi Tsuboi, Nobuhiro Kihara, and Toshikazu Takata*[a]

Abstract: A dynamic covalent approach to disulfide-containing [2]- and [3]rotaxanes is described. Symmetrical dumbbell-shaped compounds with two secondary ammonium centers and a central located disulfide bond were synthesized as components of rotaxanes. The rotaxanes were synthesized from the dumbbell-shaped compounds and dibenzo-[24]crown-8 (DB24C8) with catalysis by benzenethiol. The yields of isolated rotaxanes reached about 90% under optimized conditions. A kinetic study on the reaction forming [2]rotaxane **2a** and [3]rotaxane **3a** suggested a plausible reaction mechanism comprising several steps, including 1) initiation, 2) [2]rotaxane formation, and 3) [3]rotaxane formation. The whole reaction was found to be reversible in the presence of thiols, and thermodynamic control over product distribution was thus possible by varying the temperature, solvent, initial ratio of substrates, and concentration. The steric bulk of the end-capping groups had almost no influence on rotaxane yields, but the structure of the thiol was crucial for reaction rates. Amines and phosphines were also effective as catalysts. The structural characterization of the rotaxanes included an X-ray crystallographic study on [3]rotaxane **3a**.

Keywords: crown compounds · dynamic covalent bonds · rotaxanes · sulfur · supramolecular chemistry

Introduction

The synthesis of organic molecules has traditionally been achieved by kinetically controlled reactions that form "strong" covalent bonds. In this kind of synthesis, reagents and conditions must be chosen very carefully to avoid unfavorable bond formations. On the other hand, supramolecular chemistry, which utilizes noncovalent bonding interactions to form supramolecules under thermodynamically controlled conditions, has advanced so far that it is now possible to create various kinds of complex molecular assemblies.[1] However, in most cases, the noncovalent bonding interactions are so weak that the supramolecular assemblies disassemble into their components upon any change in conditions. Recently, chemists have opened up a new field of synthetic chemistry that exploits "dynamic" covalent bonds which can be formed and broken reversibly under thermodynamic control.[2]

[a] Prof. Dr. T. Takata, Dr. Y. Furusho, T. Oku, T. Hasegawa, A. Tsuboi, Dr. N. Kihara
Department of Applied Chemistry
Graduate School of Engineering
Osaka Prefecture University
1-1 Gakuen-cho, Sakai, Osaka 599-8531 (Japan)
Fax: (+81) 72-254-9910
E-mail: takata@chem.osakafu-u.ac.jp

Dynamic covalent chemistry has proved be a powerful way to synthesize mechanically or topologically interlocked compounds such as catenanes and rotaxanes.[3] To the best of our knowledge, Harrison reported in 1972 the first use of trityl ether bonds as dynamic covalent bonds to synthesize rotaxanes by a statistical approach.[4] Similarly, Schill et al. used trityl thioethers for the synthesis of interlocked molecules.[5] Sanders et al. employed ring-closing metathesis in 1998 to synthesize π-electron-poor/π-electron-rich[2] catenanes, and this was the first template-directed approach to interlocked molecules using dynamic covalent bonds under thermodynamically controlled conditions.[6] Leigh et al. also utilized olefin metathesis in the synthesis of "magic rings" or benzylic amide[2] catenanes having a C=C bond in each ring.[7] Additionally, Stoddart et al. demonstrated that imine bonds are very useful as dynamic covalent bonds for the construction of rotaxanes and catenanes.[8]

One of the most intriguing dynamic covalent bonds exists in nature: the thiol–disulfide interchange reaction is widely acknowledged to be important in stabilizing protein structures. Extensive mechanistic studies on thiols and disulfides by Whitesides et al. showed that i) disulfide exchange takes place efficiently under mild conditions in the presence of a catalytic amount of thiol, and ii) disulfides are stable toward many different functional groups.[9] Still et al. demonstrated that the composition of an equilibrium system of three

 DOI: 10.1002/chem.200204644

different disulfides can indeed be influenced by host–guest interactions.[10] Tam-Chang et al. demonstrated an ingenious use of disulfide bonds to make a capsule molecule.[11] Sanders et al. took advantage of the thiol–disulfide interchange reaction to make dynamic combinatorial libraries of macrocyclic disulfides.[12]

Whereas interlocked molecules such as rotaxanes[13] and catenanes[14] possessing disulfide linkages have long been known, we first utilized the reversible nature of disulfide linkages to synthesize a rotaxane in 2000.[15] We synthesized the dumbbell-shaped molecule **1a** having two secondary ammonium salt centers and a central disulfide linkage (Scheme 1). Although dibenzo-[24]crown-8 (DB24C8) is known to bind secondary dialkylammonium ions in its macroring, no complexation was observed for a solution of **1a** and DB24C8 in CD_3CN because the 3,5-di-*tert*-butylphenyl groups were too large to invade the cavity of the DB24C8 macroring, even when the solution was heated to 100 °C. On addition of a catalytic amount of benzenethiol, however, formation of [2]rotaxane **2a** and [3]rotaxane **3a** was observed, and the mixture reached equilibrium in 30 d. Thus, this small amount of benzenethiol acted as the "key" to "unlock" the disulfide bond, and thereby allowed formation of the rotaxanes. Here we describe the dynamic covalent approach to rotaxanes having disulfide linkages in detail and the structures of the rotaxanes, highlighting the reversible nature of disulfide linkages.

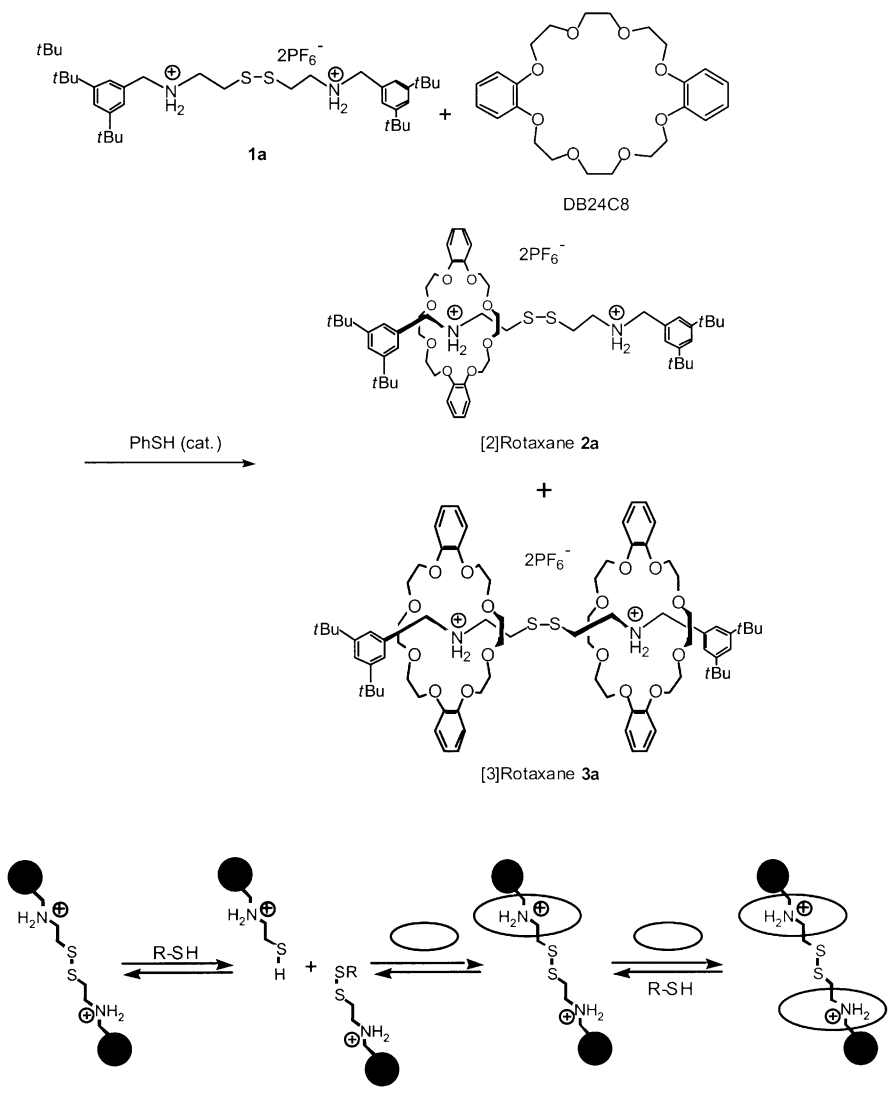

Scheme 1. Synthesis of [2]rotaxane **2a** and [3]rotaxane **3a**.

Results and Discussion

Synthesis of axles: Dumbbell-shaped axles **1** with two secondary ammonium centers and a central disulfide bond were synthesized according to Scheme 2. Benzoic acid derivatives **4** having bulky substituents were treated with thionyl chloride to form acid chlorides, which were treated with 2-aminoethanethiol to yield amides **5**. Compounds **5** were reduced with $LiAlH_4$ to the corresponding amines **6** with a central disulfide bond. Conversion of **6** to ammonium salts **1** by treatment with hydrochloric acid was followed by anion exchange with ammonium hexafluorophosphate. The analytical and spectral data of **1a–c** were consistent with the structures shown.

Synthesis of [2]- and [3]rotaxanes: A degassed solution of **1a** (0.12 mol L^{-1}) and DB24C8 (0.24 mol L^{-1})in CH_3CN was sealed in a Pyrex tube and heated at 100 °C for 12 h. No formation of rotaxanes was detected by ^1H NMR spectroscopy. This is because the dialkyl disulfide linkage is sufficiently stable, at least up to 100 °C, and because the 3,5-di-*tert*-butylphenyl end groups are far too large to pass through the DB24C8 macroring. Photoirradiation of the mixture with a Hg lamp at room temperature for 12 h yielded neither the corresponding [2]rotaxane nor the [3]rotaxane.

A catalytic amount (0.010 mol L^{-1}) of benzenethiol was added to a solution of **1a** (0.10 mol L^{-1}) and DB24C8 (0.15 mol L^{-1}) in $CDCl_3$/CD_3CN (7:3). The mixture was heated at 50 °C for 148 h and then allowed to stand at 20 °C for 240 h. The progress of the reaction was monitored by ^1H NMR spectroscopy, and the yields of [2]rotaxane **2a** and [3]rotaxane **3a** determined by

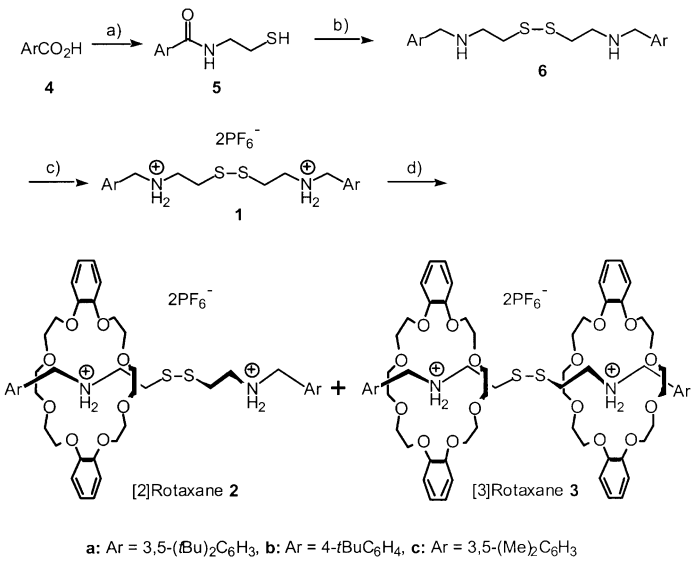

a: Ar = 3,5-(*t*Bu)$_2$C$_6$H$_3$, **b:** Ar = 4-*t*BuC$_6$H$_4$, **c:** Ar = 3,5-(Me)$_2$C$_6$H$_3$

Scheme 2. Synthesis of [2]rotaxane **2a–c** and [3]rotaxane **3a–c**. a) i) $SOCl_2$; ii) 2-aminoethanethiol, Et_3N/CH_2Cl_2. b) $LiAlH_4$/THF. c) i) HCl/MeOH; ii) NH_4PF_6 aq. d) cat. PhSH.

^{1}H NMR spectroscopy were 64 and 30%, respectively (see above). Rotaxanes **2a** and **3a** were isolated by preparative HPLC in 52 and 34% yield, respectively. Their structures were characterized by ^{1}H NMR and IR spectroscopy and FAB mass spectrometry. The yields of **2a** and **3a** reached about 90% on optimizing the reaction conditions (see below). It is noteworthy that no special manipulation to remove the catalyst is necessary: **2a** and **3a** were isolated simply by evaporation of the solvents and purification of the residue by HPLC in almost the same yields as determined by ^{1}H NMR spectroscopy. Dynamic covalent synthesis using olefin metathesis requires quenching of the catalysts to isolate the products. When imine linkages are employed as dynamic covalent bonds, it is necessary to convert the imine bonds to amine bonds for product isolation, since imine metathesis is a fast and reversible process at room temperature. The thiol–disulfide interchange reaction is slow enough to isolate rotaxanes in the presence of a thiol catalyst, but fast enough to complete the reactions within a reasonable timescale. This is advantageous in ensuring facile workup.

Structures of [2]- and [3]rotaxanes: The ^{1}H NMR spectroscopic data of the rotaxanes revealed significant chemical shifts relative to the separate axle and ring components. The ^{1}H NMR spectra of **2a**, **3a**, and a mixture of **1a** and DB24C8 recorded at 20 °C are shown in Figures 1 and 2. The signal of the *t*Bu protons of **3a** shifted to higher field ($\Delta\delta \approx -0.1$ ppm) relative to **1a**. The upfield shift is accounted for by the shielding effect of the benzene rings of the DB24C8 component. The signals of the benzylic protons of **3a** shifted to lower field relative to **1a** ($\Delta\delta \approx +0.4$ ppm). Such a downfield shift of benzylic protons with neighboring secondary ammonium groups has been observed in most (pseudo)rotaxanes consisting of crown ethers and secondary ammonium salts.[16] This is attributed to the CH···O hydrogen-bonding interaction between the benzylic protons and the oxygen atoms of the crown ether.

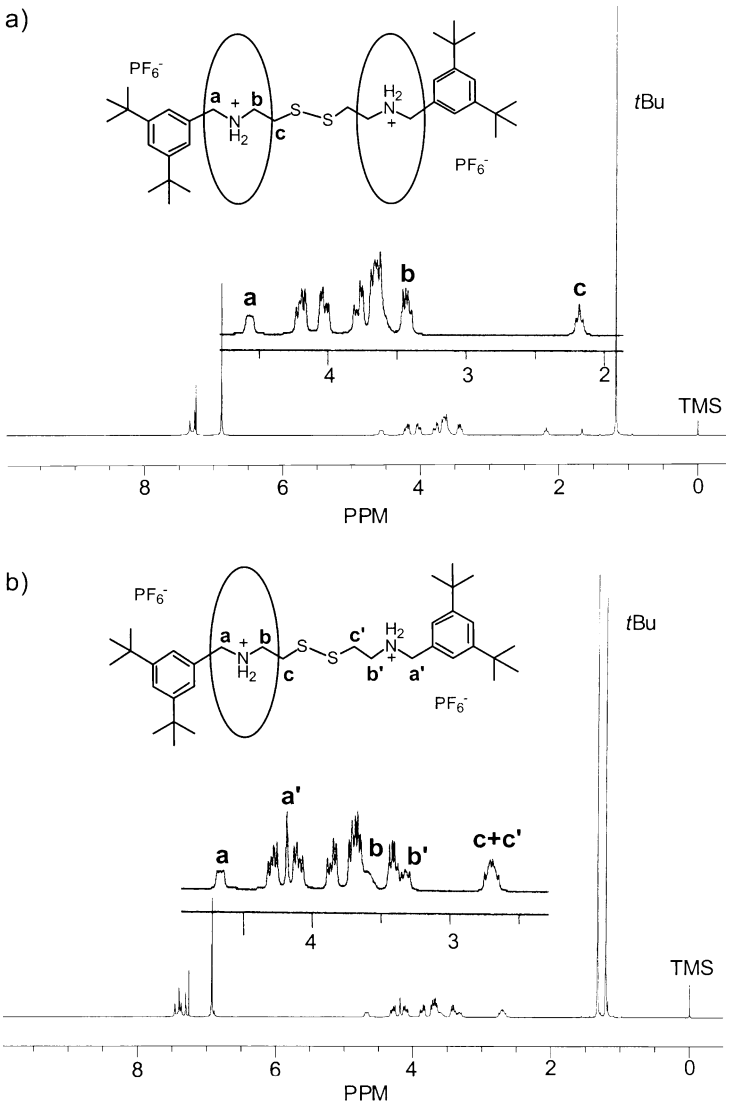

Figure 1. ^{1}H NMR spectra ($CDCl_3$, 270 MHz) of a) [3]rotaxane **3a** and b) [2]rotaxane **2a**. The rings in the structural formula denote DB24C8.

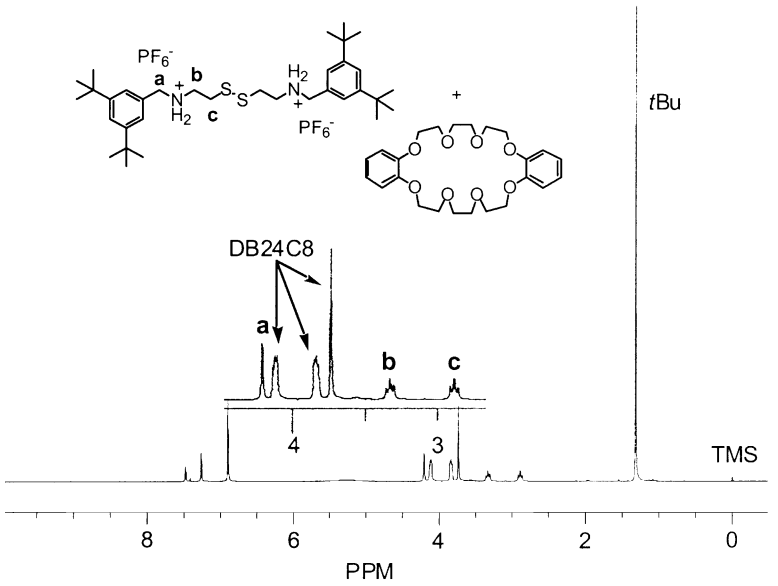

Figure 2. ^{1}H NMR spectrum ($CDCl_3/CD_3CN$ (7/3), 270 MHz) of a mixture of axle **1a** and DB24C8.

The ^{1}H NMR spectrum of [2]rotaxane **2a** showed temperature-dependent behavior. The signals of most protons of the dumbbell component were split into two peaks at room temperature, because the shuttling behavior of **2a** is slower than the ^{1}H NMR timescale. The signal of the *t*Bu protons of the half of the dumbbell unit encircled DB24C8 shifted to higher field, while those of the benzylic protons shifted to lower field, as in the case of **3a**. The signals of the other half of the dumbbell unit, which is not encircled by DB24C8, did not shift compared to those of the axle **1a**. The signals specific to **2a** and **3a**, such as those of *t*Bu and benzylic protons, were used to monitor the the synthesis of the rotaxanes, as described below.

X-ray crystal structure analysis of **3a** revealed an interlocked structure (Figure 3a) which resembles that of the disulfide-containing [3]rotaxane of Busch et al.[13] Each DB24C8 macroring adopts a folded U-shaped conformation, with the NH_2^+ inserted approximately axially through its center. The two DB24C8 macrorings are folded together to form a "tennis ball"-like assembly.[17] Complex stabilization is achieved by a combination of $N^+-H\cdots O$ and $C-H\cdots O$ hydrogen bonds. The disulfide group is surrounded by the four catechol rings of DB24C8. Inspection of the solid-state structure reveals no interactions between the disulfide moiety and the DB24C8 macrorings. The structural parameters of the disulfide moiety (Figure 3b) are reminiscent of those of dimethyl disulfide, as determined by gas-phase electron diffraction:[18] the S–S and C–S bond lengths of **3a** are 2.035(1) and 1.818(4)/1.812(4) Å, respectively, while those of dimethyl disulfide are 2.022(3) and 1.806(2) Å, respectively; the S-S-C bond angles of **3a** are 104.5(1) and 102.9(1)°, values similar to those of dimethyl disulfide (104.1(3)°); the disulfide moiety of **3a** adopts a *gauche* conformation with a C-S-S-C dihedral angle of 82.2(5)°, which is also very close to that of dimethyl disulfide (83.9(9)°).

Reaction mechanism and reversible cleavage/recombination of the disulfide linkage: A catalytic amount (0.010 mol L^{-1}) of benzenethiol was added to a solution of **1a** (0.10 mol L^{-1}) and DB24C8 (0.20 mol L^{-1}) in CD_3CN. The mixture was heated at 50 °C, and the progress of the reaction was monitored by ^{1}H NMR spectroscpy. The time courses of the yields of **2a** and **3a** are shown in Figure 4. Soon after initiation, **2a** was formed, and the yield of **2a** gradually increased. The yield of **2a** reached its maximum value (69 %) after 4 h, and then eventually decreased. The signals of **3a** appeared after about 4 h, and the yield of **3a** increased with a concomitant decrease in the yield of **2a**. The system reached equilibrium after about 36 h, where the yields of **2a** and **3a** were 29 and 65 %, respectively.

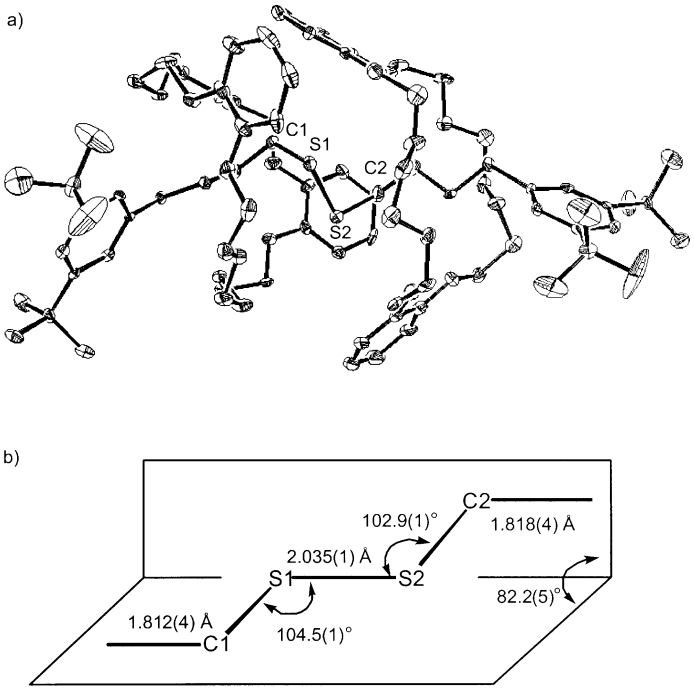

Figure 3. X-ray crystallographic structure of [3]rotaxane **3a**. a) ORTEP plot of **3a**. Thermal ellipsoids are scaled to the 50 % probability level. b) Schematic diagram of the structure around the disulfide linkage of **3a**.

These results suggest a possible reaction mechanism (Scheme 3). The reaction is initiated by the nucleophilic attack of benzenethiol at the disulfide linkage, which results in thiol **A** and benzenethiol-terminated disulfide **B** [Eq. (1)]. Then DB24C8 rapidly threads onto **A** and **B** to form pseudorotaxanes **A**·DB24C8 and **B**·DB24C8 [Eqs. (2) and (3)]. The nucleophilic displacement of the phenylthio group in **A**·DB24C8 by **B** gives [2]rotaxane **2** and benzenethiol

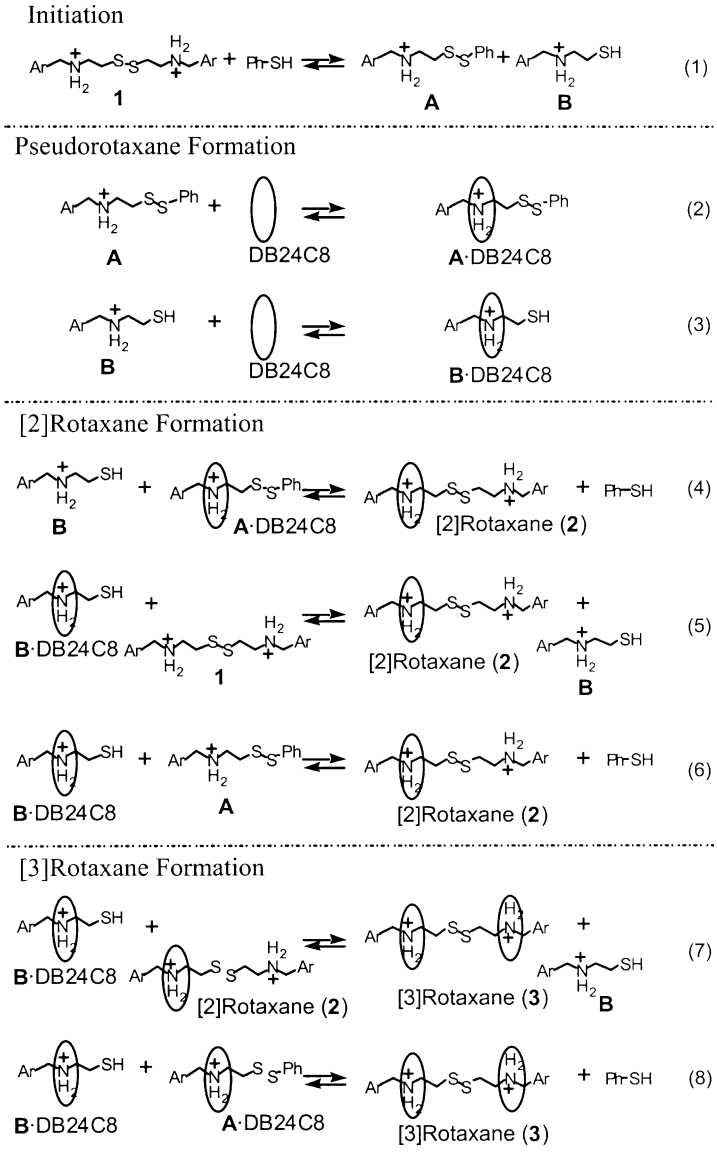

Scheme 3. Possible reaction mechanism.

[Eq. (4)]. Pseudorotaxane **B**·DB24C8 nucleophilically attacks **1** or **A** to afford **2** [Eqs. (5) and (6)]. [3]Rotaxane **3** is formed by reaction of **B**·DB24C8 and **2**, or of **B**·DB24C8 and **A**·DB24C8 [Eqs. (7) and (8)].

The reaction mixture was then cooled and kept at room temperature (Figure 4). After 80 h (240 h after initiation), the system reached another equilibrium state, in which the yields of **2a** and **3a** were 15 and 81 %, respectively. Since the main driving force for rotaxane formation is the exothermic hydrogen-bonding interaction between the secondary ammonium group and DB24C8, the equilibrium shifted to the [3]rotaxane side on lowering the reaction temperature. Raising the temperature again to 50 °C returned the equilibrium to the original state. These results demonstrate that the whole process is reversible and that the yields of the rotaxanes can be changed under thermodynamic control.

Thermodynamic control: Since the hydrogen-bonding interaction is the main driving force for rotaxane formation, the

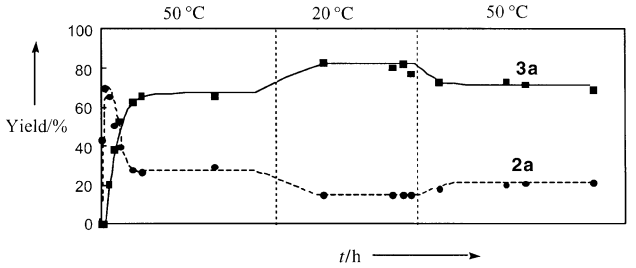

Figure 4. Time course of the yields of [2]rotaxane **2a** and [3]rotaxane **3a**. [**1a**] = 0.10 mol L^{-1}, [DB24C8] = 0.20 mol L^{-1}, [PhSH] = 0.010 mol L^{-1} in CD_3CN.

equilibrium is affected by solvent polarity, especially by donor numbers (DN).[16, 19, 20] We recently reported that dielectric constants also influence the association constants of pseudorotaxane formation in addition to DN.[21] The yields of the rotaxanes are expected to increase when solvents with lower DN are used. However, the use of $CDCl_3$, which has a lower DN (4.0) than CD_3CN (DN 14.1) as co-solvent did not change the yields of the rotaxanes (Table 1, entries 3 and 4). A

Table 1. Effect of solvent on the formation of [2]rotaxane **2a** and [3]rotaxane **3a** from **1a** and DB24C8 (cat. 0.1 mol L^{-1} PhSH).

	Concentration/mol L^{-1}			Yield/%[a]	
Entry	Solvent	**1a**	DB24C8	*T*/°C	**2a**	**3a**
1	CD_3CN	0.10	0.20	50	29	65
2				20	15	81
3	$CDCl_3/CD_3CN$ 7:3	0.10	0.20	50	24	64
4				20	15	77
5	$CDCl_3/CD_3OD$ 1:1	0.10	0.20	50	37	60
6	CD_3NO_2	0.10	0.20	50	17	83
7	DMF	0.10	0.30	50	< 10	0

[a] Determined by ^{1}H NMR spectroscopy at equilibrium (error ca. 5 %).

mixture of $CDCl_3$ and CD_3OD with a higher DN than CD_3CN shifted the equilibrium to the [2]rotaxane side (entry 5). [D_3]Nitromethane (DN 2.7) gave the highest yield of [3]rotaxane **3a** (83 %, even at 50 °C, entry 6). The use of DMF (DN 26.6) resulted in a dramatic decrease in yield (entry 7). Thus, the solvent effects on the yields of the rotaxanes could, to a certain extent, be accounted for by donor numbers in this system.

The effects of the ratio of DB24C8 to **1a** were examined (Table 2). When equimolar amounts of DB24C8 and **1a** were employed, **2a** was obtained preferentially at 50 °C (entry 1). Increasing the DB24C8/**1a** ratio dramatically shifted the equilibrium to **3a** (entries 2–4). As described above, con-

Table 2. Effect of the initial ratio of DB24C8 to **1a** ([**1a**] = 0.1 mol L^{-1}, cat. 0.01 mol L^{-1} PhSH, $CDCl_3/CD_3CN$, 50 °C).

		Yield/ %[a]	
Entry	[DB24C8]/mol L^{-1}	**2a**	**3a**
1	0.10	65	10
2	0.15	69	26
3	0.20	29	65
4	0.30	12	88
5	0.40	10	82

[a] Determined by ^{1}H NMR spectroscpy at equilibrium (error ca. 5 %).

ducting the reaction at a DB24C8/**1a** ratio of 2 yielded preferentially **3a** (entry 3). Using three equivalents of DB24C8 gave the highest yields of **3a** (entry 4). However, the use of four equivalents of DB24C8 resulted in a lower yield of **3a** (entry 5). The decrease in the yield of **3a** when an excess of DB24C8 is used is attributed to the increased polarity of the reaction mixture caused by DB24C8 itself, which diminishes the association constant for pseudorotaxane formation, as reported previously.[21]

Increasing the concentrations of **1a** (0.710 mol L^{-1}) and DB24C8 (1.42 mol L^{-1}) in $CDCl_3/CD_3CN$ (1:1) gave **3a** in 89% yield at 20 °C, while the reaction carried out at initial concentrations of [**1a**] = 0.10 mol L^{-1} and [DB24C8] = 0.20 mol L^{-1} afforded **3a** in 77% yield at 20 °C (Table 3). In this case, the advantage of the high initial concentrations exceeded the drawback of the increased polarity of the reaction system. Thus, the product distribution of this reaction can easily be controlled by changing the initial concentrations.

Table 3. Effect of concentration on the formation of [2]rotaxane **2a** and [3]rotaxane **3a** (cat. 0.01 mol L^{-1} PhSH).

		Concentration/mol L^{-1}			Yield/%[a]	
Entry	Solvent	**1a**	DB24C8	*T*/°C	**2a**	**3a**
1	$CDCl_3/CD_3CN$ 7:3	0.10	0.20	50	24	64
2				20	15	77
3	$CDCl_3/CD_3CN$ 1:1	0.710	1.42	20	10	89

[a] Determined by ^{1}H NMR spectroscopy at equilibrium (error ca. 5%).

Effect of end-capping groups: Three axles **1a–c** were employed for the synthesis of rotaxanes to examine the steric effects of end-capping groups on the yield (Table 4). The axles having less hindered endcapping groups (**1b** and **1c**) afforded the corresponding [2]rotaxanes **2b** and **2c** and [3]rotaxanes **3b** and **3c** in almost the same yields. Thus, the steric effect of end-capping groups appears relatively small from the viewpoint of rotaxane yield.

Table 4. Effect of end caps on the yields of [2]rotaxanes **2** and [3]rotaxanes **3** ([**1a**] = 0.1 mol L^{-1}, [DB24C8] = 0.2 mol L^{-1}, cat. 0.01 mol L^{-1} PhSH, CD_3CN).

Axle	*T*/°C	Yield/%[a]	
		2	**3**
1a	50	29	65
	20	15	81
1b	50	19	63
	20	11	81
1c	50	22	61
	20	11	79

[a] Determined by ^{1}H NMR spectroscopy at equilibrium (error ca. 5%).

Effect of thiols: To evaluate the effect of the thiol catalyst, thiol **7a**[22] and *t*BuSH were used as initiators. The use of **7a** caused a retarded reaction rate (Figure 5). The yield of **2a**, evaluated by ^{1}H NMR spectroscopy, reached a maximum value of 95% 33 h after initiation, indicative of a much slower rate than that obtained with PhSH. This decrease in reaction rate is attributed to the lack of contributions from Equations (4), (6), and (8) in Scheme 3. This slow rate makes it easier to isolate [2]rotaxanes during the period in which their yields peak. In a separate experiment under the same conditions, **2a** was indeed isolated in 89% yield 40 h after initiation. When *t*BuSH was employed as an initiator, the reaction rate was much slower than those obtained with PhSH and **7a**. The system did not reach equilibrium, even after 300 h. This is attributable to the lack of contributions from Equations (4), (6), and (8) in Scheme 3, as well as to the low nucleophilicity of *t*BuSH because of the steric hindrance of the *tert*-butyl group. Note that **2a** could be isolated in 89% yield under "kinetic" conditions.

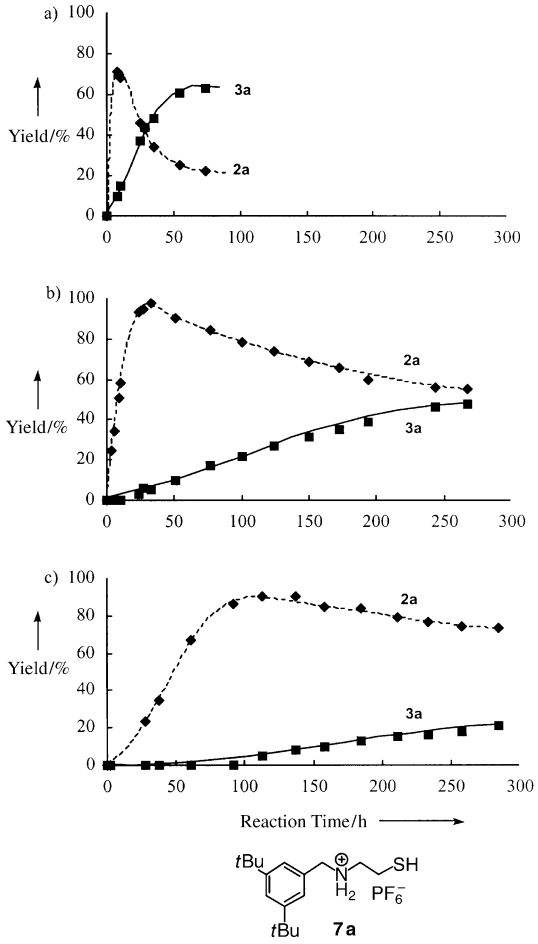

Figure 5. Time course of the yields of [2]rotaxane **2a** and [3]rotaxane **3a** with a) PhSH, b) **7a**, and c) *t*BuSH as initiator. [**1a**] = 0.10 mol L^{-1}, [DB24C8] = 0.20 mol L^{-1}, [initiator] = 0.010 mol L^{-1} in $CDCl_3/CD_3CN$ 7:3 at 50 °C.

Initiators other than thiols: Disulfide linkages can be cleaved by various nucleophiles other than thiols.[23] To confirm the efficiency of thiol catalysts, we examined 4-nitrophenol, diethylamine, and hexamethylphosphoric triamide (HMPT) as initiators (Table 5). 4-Nitrophenol did not react with **1a** at 50 °C, even after 60 h (entry 2). Diethylamine catalyzed the rotaxane synthesis, and the yields of **2a** and **3a** were 25 and 4%, respectively, at 50 °C after 67 h (entry 3), although the

Table 5. Effect of catalysts on the yields of [2]rotaxane **2a** and [3]rotaxane **3a** ([**1a**] = 0.1 mol L^{-1}, [DB24C8] = 0.2 mol L^{-1}, [cat.] = 0.01 mol L^{-1}, CD_3CN, 20 °C).

Catalyst	t/h[a]	Yield/ %[b] **2**	**3**
PhSH	55	25	61
4-Nitrophenol	60	0	0
Et_2NH	67	25	4
HMPT	54	60	24

[a] All reactions did not reach equilibrium. [b] Determined by ^{1}H NMR spectroscopy (error ca. 5 %).

reaction rate was as slow as that with *t*BuSH. HMPT also reacted with **1a** to catalyze the formation of **2a** and **3a** (entry 4).[24] Thus, amines and phosphines are potential catalysts for rotaxane synthesis utilizing the reversible nature of disulfide linkages.

Conclusion

Symmetrical dumbbell-shaped compounds **1** with two ammonium centers and a central disulfide bond were designed with the aim of investigating the utility of disulfide linkages as dynamic covalent bonds for rotaxane synthesis. Compound **1** and DB24C8 reacted with catalysis by benzenethiol to afford [2]- and [3]rotaxanes in good yields. Kinetic studies on the reaction suggested a mechanism involving several steps such as initiation, [2]rotaxane formation, and [3]rotaxane formation. Since the whole reaction is fully reversible, product distributions were controllable under thermodynamic conditions by changing temperature, solvent, initial ratios of substrates, and concentrations. The yield of [3]rotaxane **3a** reached up to 89 %. On the other hand, [2]rotaxane **2a** was isolated in 89 % yield by changing the structure of the thiol catalyst to decelerate the reaction rate. Thus, disulfide linkages were shown to be effective as dynamic covalent bonds for the construction of rotaxanes. We believe that more complicated supramolecules such as catenanes and knots can be synthesized by means of thiol–disulfide interchange reactions. since these proceed well under mild conditions and can tolerate many functional groups.[25]

Experimental Section

General: Melting points were measured on a Yanagimoto micro melting-point apparatus and were uncorrected. IR spectra were recorded on a JASCO FT-IR model 230 spectrometer. ^{1}H NMR spectra were recorded on JEOL JNM-GX-270 and JNM-L-400 spectrometers in $CDCl_3$ with tetramethylsilane as an internal reference. FABMS measurements were performed on a Finnigan TSQ-70 instrument. For preparative HPLC, a JAICO LC-908 system using columns JAIGEL 1 (20 mm∅ × 600 mm) and JAIGEL 2 (20 mm∅ × 600 mm) was employed. X-ray diffraction was carried out on a Rigaku R-AXIS RAPID imaging plate system. All reagents used were commercially available, except for **4a**, which was prepared according to the literature procedure.[21]

Representative procedure for the synthesis of amide 5: A solution of 3,5-di-*tert*-butylbenzoic acid[21] (**4a**, 5.56 g, 23.7 mmol) in $SOCl_2$ (13 mL) was stirred overnight at 50 °C. Then the mixture was concentrated in vacuo. The remaining $SOCl_2$ was removed as an azeotropic mixture with benzene to give the corresponding acid chloride. A solution of the acid chloride in Et_2O (15 mL) was slowly added to a solution of 2-aminoethanethiol (2.26 g, 29.3 mmol) and Et_3N (4.2 mL, 30 mmol) in CH_2Cl_2 (115 mL). The mixture was stirred for 1 h at room temperature, washed with 1M HCl (20 mL × 3), and treated successively with brine, anhydrous $MgSO_4$, and evaporated to dryness to give amide **5** as a white solid.

Compound **5a**: quantitative; m.p. 188–191 °C; ^{1}H NMR (270 MHz, $CDCl_3$, 23 °C): δ = 7.59 (m, 3H, ArH), 6.55 (s, 1H, NH), 3.64 (q, J = 6.5 Hz, 2H, CH), 2.80 (dt, J = 8.4, 6.5 Hz, 2H, CH), 1.42 (t, 1H, J = 8.4 Hz, SH), 1.35 (s, 18H, *t*Bu); IR (KBr): $\tilde{\nu}$ = 3249 (N–H), 2570 (S–H), 1633 (C=O), 1595 (C=C), 1543 cm^{-1} (C=C).

Compound **5b**: quantitative; ^{1}H NMR ($CDCl_3$, 270 MHz, 23 °C): δ = 7.74 (d, J = 4.1 Hz, 2H, ArH), 7.70 (d, J = 4.1 Hz, 2H, ArH), 6.59 (s, 1H, NH), 3.64 (q, J = 6.2 Hz, 2H, CH_2), 2.79 (dt, J = 8.4, 6.2 Hz, 2H, CH_2), 1.40 (t, J = 8.4 Hz, 1H, SH), 1.34 (s, 9H, *t*Bu); IR (KBr): $\tilde{\nu}$ = 3246 (N–H), 2570 (S–H), 1633 (C=O), 1595 (C=C), 1545 cm^{-1} (C=C).

Compound **5c**: 94 %; ^{1}H NMR ($CDCl_3$, 270 MHz, 23 °C): δ = 7.38 (s, 2H, ArH), 7.12 (s, 1H, ArH), 6.70 (s, 1H, NH), 3.62 (q, J = 6.2 Hz, 2H, CH_2), 2.74 (dt, J = 8.6, 6.2 Hz, 2H, CH_2), 2.34 (s, 6H, CH_3), 1.41 (t, J = 8.6 Hz, 1H, SH); IR (KBr): $\tilde{\nu}$ = 3311 (N–H), 2561 (S–H), 1639 (C=O), 1601 (C=C), 1539 cm^{-1} (C=C).

Representative procedure for the synthesis of amine 6: Compound **5a** was added to a suspension of $LiAlH_4$ (80 %, 1.32 g, 27.8 mmol) in THF (40 mL). The mixture was heated under reflux for 17 h. Saturated aqueous sodium sulfate solution was then added carefully to the mixture to form a white precipitate, which was removed by suction filtration. The filtrate was evaporated to dryness. The residue was subjected to column chromatography on silica gel (chloroform) to afford the amine **6a** as a colorless oil.

Compound **6a**: 88 %; oil; ^{1}H NMR (400 MHz, $CDCl_3$, 23 °C): δ = 7.32 (t, J = 1.6 Hz, 2H, ArH), 7.15 (d, J = 1.6 Hz, 4H, ArH), 3.80 (s, 4H, CH_2), 2.98 (t, J = 6.0 Hz, 4H, CH_2), 2.85 (t, J = 6.0 Hz, CH_2), 1.33 (s, 36H, *t*Bu); IR (KBr): $\tilde{\nu}$ = 3604 (N–H), 1599 (C=C), 1476 (C=C), 1458 cm^{-1} (C=C).

Compound **6b**: quantitative; ^{1}H NMR($CDCl_3$, 270 MHz, 23 °C): δ = 7.43–7.20 (m, 8H, ArH), 3.76 (s, 4H, CH_2), 2.93 (t, J = 5.9 Hz, 4H, CH_2), 2.81 (t, J = 5.9 Hz, 4H, CH_2), 1.31 (s, 18H, *t*Bu); IR (KBr): $\tilde{\nu}$ = 3288 (N–H), 1511 (C=C), 1458 cm^{-1} (C=C).

Compound **6c**: 99 %; ^{1}H NMR ($CDCl_3$, 270 MHz, 23 °C): δ = 6.85 (m, 6H, ArH), 3.72 (s, 2H, CH_2), 2.81 (t, J = 5.9 Hz, 4H, CH_2), 2.68 (t, J = 5.9 Hz, 4H, CH_2), 2.31 (s, 12H, CH_3); IR (KBr): $\tilde{\nu}$ = 3306 (N–H), 1606 (C=C), 1457 cm^{-1} (C=C).

Representative procedure for the synthesis of dumbbell 1: A solution of **6a** (3.00 g, 5.13 mmol) in methanol/conc. HCl (30/7 mL) was stirred for 45 min. Water (50 mL) was added to the solution to form a white precipitate, which was collected by suction filtration. The white solid was washed with water, dried under reduced pressure, and reprecipitated from MeOH/water to give the corresponding hydrochloric acid salt of **6a** as a white solid. The hydrochloric acid salt (1.34 g, 2.04 mmol) was dissolved in MeOH (15 mL). A solution of ammonium hexafluorophosphate (1.93 g, 11.8 mmol) in water (10 mL) was slowly added to the methanolic solution to form a white precipitate. Water was added to the resulting solution until no further precipitation occurred. The white solid was collected by suction filtration, washed with water, dried under reduced pressure, and recrystallized from water/ethanol to afforded the dumbbell **1a**.

Compound **1a**: 95 %; needlelike crystals; m.p. (decomp): 225–230 °C; ^{1}H NMR (270 MHz, CD_3CN, 23 °C): δ = 7.55 (t, J = 1.6 Hz, 2H, ArH), 7.31 (d, J = 1.6 Hz, 4H, ArH), 4.38 (brs, 4H, NH_2), 4.18 (s, 4H, CH_2), 3.34 (t, J = 6.8 Hz, 4H, CH_2), 2.92 (t, J = 6.8 Hz, 4H, CH_2), 1.33 (s, 36H, *t*Bu); IR (KBr): $\tilde{\nu}$ = 3237 (N–H), 1604 (C=C), 839 (P–F), 557 cm^{-1} (P–F); FABMS (matrix: *m*NBA): m/z: 558.7 $[M-2PF_6]^+$; elemental analysis (%) calcd for $C_{34}H_{58}F_{12}N_2P_2S_2 \cdot H_2O$ (848.90): C 47.11, H 6.98, N 3.23; found: C 47.39, H 6.73, N 3.26.

Compound **1b**: 86 %; white crystals; m.p. (decomp): 232–235 °C; ^{1}H NMR (270 MHz, CD_3CN, 23 °C): δ = 7.52 (d, J = 8.1 Hz, 4H, ArH), 7.40 (d, J = 8.1 Hz, 4H, ArH), 5.97 (brs, 4H, NH_2), 4.20 (s, 4H, CH_2), 3.36 (t, J = 6.9 Hz, 4H, CH_2), 2.93 (t, J = 6.9 Hz, 4H, CH_2), 1.32 (s, 18H, *t*Bu); IR (KBr): $\tilde{\nu}$ = 3253 (N–H), 1586 (C=C), 839 (P–F), 557 cm^{-1} (P–F); FABMS (matrix: *m*NBA): m/z: 591.0 $[M-PF_6]^+$, 445.0 $[M-2PF_6]^+$; elemental

analysis (%) calcd for $C_{26}H_{42}F_{12}N_2P_2S_2$ (736.69): C 42.39, H 5.75, N 3.80; found: C 42.66, H 5.61, N 3.78.

Compound **1c**: 46%; white crystals; m.p. (decomp): 215–217 °C; ^{1}H NMR (270 MHz, [D$_6$]DMSO, 23 °C): $\delta = 8.80$ (brs, 4H, NH_2), 7.08 (s, 6H, ArH), 4.11 (s, 4H, CH_2), 3.23 (t, $J = 6.8$ Hz, 4H, CH_2), 2.96 (t, $J = 6.8$ Hz, 4H, CH_2), 2.30 (s, 12H, CH_3); IR (KBr): $\tilde{\nu} = 3247$ (N–H), 1611 (C=C), 1467 (C=C), 839 (P–F), 557 cm^{-1} (P–F); FABMS (matrix: *m*NBA): *m/z*: 534.6 $[M - PF_6]^+$, 391.6 $[M - 2PF_6{+}H]^+$; elemental analysis (%) calcd for $C_{22}H_{34}N_2S_2 \cdot 1.9PF_6 \cdot 0.1H_2PO_4$ (680.58): C 39.10, H 5.10, N 4.15; found: C 39.21, H 4.79, N 4.26.

Representative procedure for the synthesis of [2]rotaxane 2 and [3]rotaxane 3: A catalytic amount of benzenethiol (1.0 μL, 0.01 mmol) was added to a solution of **1a** (85 g, 0.10 mmol) and DB24C8 (69 g, 0.15 mmol) in $CD_3CN/CDCl_3$ (0.3/0.7 mL). The solution was sealed in an NMR tube (∅ 5 mm), which was heated at 50 °C for 6 d and cooled and kept at room temperature for 10 d. The progress of the reaction was monitored by ^{1}H NMR spectroscopy. The mixture was evaporated to dryness. The residue was subjected to preparative HPLC to afford **2a** and **3a**.

Compound **2a**: ^{1}H NMR (270 MHz, $CDCl_3$, 23 °C): $\delta = 7.46$ (t, $J = 1.6$ Hz, 1H, ArH), 7.40 (d, $J = 1.6$ Hz, 2H, ArH), 7.39 (brs, 2H, NH_2 complexed with DB24C8), 7.37 (t, $J = 1.6$ Hz, 1H, ArH), 7.30 (d, $J = 1.6$ Hz, 2H, ArH), 6.92 (s, 8H, ArH), 4.67 (m, 4H, CH_2), 4.35–4.05 (m, 10H, CH_2), 3.92–3.25 (m, 20H, CH_2), 2.70 (m, 4H, CH_2), 1.33 (s, 18H, *t*Bu), 1.21 (s, 18H, *t*Bu), the signal of NH_2 uncomplexed with DB24C8 was not observed; IR (KBr): $\tilde{\nu} =$ 3155 (N–H), 1597 (C=C), 1506 (C=C), 845 (P–F), 558 cm^{-1} (P–F); FABMS (matrix: *m*NBA): *m/z*: 1006 $[M - 2PF_6]^+$; elemental analysis (%) calcd for $C_{58}H_{90}F_{12}N_2O_8P_2S_2$ (1297.40): C 53.69, H 6.99, N 2.16, S 4.94; found: C 53.17, H 6.97, N 2.45, S 4.83.

Compound **2b**: ^{1}H NMR (270 MHz, $CDCl_3$, 23 °C): $\delta = 7.47$ (d, $J = 8.6$ Hz, 2H, ArH), 7.38(d, $J = 8.6$ Hz, 2H, ArH), 7.33 (brs, 2H, NH_2 complexed with DB24C8), 7.28(d, $J = 8.6$ H, 2H, ArH), 7.22 (d, $J = 8.6$ Hz, 2H, ArH), 6.88 (m, 8H, ArH), 4.7 (brs, 2H, NH_2 uncomplexed with DB24C8), 4.59 (m, 2H, CH_2), 4.32–3.97 (m, 10H, CH_2), 3.95–3.40 (m, 18H, CH_2), 3.13 (t, $J = 7.0$ Hz, 2H, CH_2), 2.81 (m, 4H, CH_2), 1.28 (s, 9H, *t*Bu), 1.25 (s, 9H, *t*Bu); IR (KBr): $\tilde{\nu} = 3135$ (N–H), 1595 (C=C), 1506 (C=C), 843 (P–F), 558 cm^{-1} (P–F); FABMS (matrix: *m*NBA): *m/z*: 894 $[M - 2PF_6]^+$; elemental analysis (%) calcd for $C_{50}H_{74}N_2O_8S_2 \cdot 2H_2PO_4 \cdot$ (1185.19): C 55.13, H 7.22, N 2.57; found: C 54.97, H 7.00, N 2.37.

Compound **2c**: m.p. 68–70 °C; ^{1}H NMR (270 MHz, $CDCl_3$, 23 °C): $\delta = 7.28$ (brs, 2H, NH_2 complexed with DB24C8), 7.15 (s, 2H, ArH), 6.98 (s, 1H, ArH), 6.95–6.80 (m, 11H, ArH), 6.10 (brs, 2H, NH_2 uncomplexed with DB24C8), 4.52 (m, 2H, CH_2), 4.30–4.00 (m, 10H, CH_2), 3.95–3.40 (m, 18H, CH_2), 3.23 (t, $J = 7.3$ Hz, 2H, CH_2), 2.79 (m, 4H, CH_2), 2.29 (s, 6H, CH_3), 2.15 (s, 6H, CH_3); IR (KBr): $\tilde{\nu} = 3135$ (N–H), 1595 (C=C), 1506 (C=C), 843 (P–F), 558 cm^{-1} (P–F); FABMS (matrix: *m*NBA): *m/z*: 837 $[M - 2PF_6]^+$; elemental analysis (%) calcd for $C_{46}H_{66}N_2O_8S_2 \cdot PF_6 \cdot H_2PO_4$ (1129.09): C 51.10, H 6.34 N 2.59; found: C 51.14, H 6.57, N 2.43.

Compound **3a**: m.p. 207–208 °C; ^{1}H NMR (270 MHz, $CDCl_3$, 23 °C): $\delta =$ 7.35 (s, 2H, ArH), 7.34 (brs, 4H, NH_2), 7.28 (s, 4H, ArH), 6.89 (s, 16H, ArH), 4.57 (m, 4H, CH_2), 4.30–3.95 (m, 8H, CH_2), 3.85–3.30 (m, 20H, CH_2), 2.18 (t, $J = 6.2$ Hz, 4H), 1.18 (s, 36H, *t*Bu); IR (KBr): $\tilde{\nu} = 3164$ (N–H), 1596 (C=C), 1506 (C=C), 843 (P–F), 558 cm^{-1} (P–F); FABMS (matrix: *m*NBA): *m/z*: 1454 $[M - 2PF_6]^+$; elemental analysis (%) calcd for $C_{82}H_{122}F_{12}N_2O_{16}P_2S_2$ (1745.91): C 56.41, H 7.04, N 1.60; found: C 56.14, H 7.16, N 1.44.

Compound **3b**: m.p. 186–188 °C; ^{1}H NMR (270 MHz, $CDCl_3$, 23 °C): $\delta =$ 7.28 (brs, 4H, NH_2), 7.24 (d, $J = 8.6$ Hz, 4H, ArH), 7.18 (d, $J = 8.6$ Hz, 4H, ArH), 6.83 (s, 8H, ArH), 4.55 (m, 4H, ArH), 4.25–3.95 (m, 16H, CH_2), 3.90–3.45 (m, 36H, CH_2), 2.45 (t, $J = 6.8$ Hz, 4H), 1.23 (s, 18H, *t*Bu); IR (KBr): $\tilde{\nu} = 3178$ (N–H), 1593 (C=C), 1506 (C=C), 845 (P–F), 557 cm^{-1} (P–F); FABMS (matrix: *m*NBA): *m/z*: 1488 $[M - PF_6]^+$; elemental analysis (%) calcd for $C_{74}H_{106}F_{12}N_2O_{16}P_2S_2$ (1633.70): C 54.40, H 6.54, N 1.74; found: C 54.39, H 6.64, N 1.74.

Compound **3c**: m.p. 223–224 °C; ^{1}H NMR (270 MHz, [D$_6$]DMSO, 23 °C): $\delta = 7.17$ (brs, 4H, NH_2), 7.00–6.85 (m, 22H, ArH), 4.41 (m, 4H, CH_2), 4.20–3.90 (m, 16H, CH_2), 3.80–3.40 (m, 36H, CH_2), 2.27 (t, $J = 6.8$ Hz, 4H), 2.13 (s, 12H, CH_3); IR (KBr): $\tilde{\nu} = 3154$ (N–H), 1594 (C=C), 840 (P–F), 557 cm^{-1} (P–F); FABMS (matrix: *m*NBA): *m/z*: 1432 $[M - PF_6]^+$; elemental analysis (%) calcd for $C_{70}H_{98}F_{12}N_2O_{16}P_2S_2 \cdot H_2O$ (1577.59): C 52.69, H 6.32, N 1.76, S 4.02; found: C 52.70, H 6.21, N 1.94, S 4.26.

X-ray crystallographic analysis of [3]rotaxane (3a): Single crystals suitable for X-ray analysis were grown by recrystallization from MeOH. Crystal data: $C_{82}H_{122}F_{12}N_2O_{16}P_2S_2 \cdot 2MeOH$, $M = 1810.0$, triclinic, $a = 161215(6)$, $b = 17.1050(6)$, $c = 17.3503(6)$ Å, $\alpha = 106.506(1)$, $\beta = 95.903(2)$, $\gamma =$ $90.168(2)^\circ$, $V = 4560.4(3)$ Å^3, space group $P\bar{1}$, $Z = 2$, $\rho = 1.318$ g cm^{-3}, $\mu(Mo_{K\alpha}) = 0.183$ mm^{-1}, $F(000) = 1808$. 20398 independent reflections ($2\theta < 55^\circ$) were collected with a Rigaku R-AXIS-RAPID imaging plate system, equipped with a rotating anode generator, at 103 K using ω scans and graphite-monochromatized $Mo_{K\alpha}$ radiation. Refinement was carried out for reflections with $F^2 > 3\sigma(F^2)$. The structure was solved by a direct method (SIR97). *wR*, GOF, and *R* were based on *F*, which was set to zero for negative values. The threshold expression of $F^2 > 2\sigma(F^2)$ was used only for calculating the *R* factor. *wR*, GOF, and *R* were 0.058, 0.090, and 1.000, respectively. Calculations were carried out with the CrystalStructure package (version 2.0). CCDC-196932 contains the supplementary crystallographic data for this paper. These data can be obtained free of charge via www.ccdc.cam.ac.uk/conts/retrieving.html (or from the Cambridge Crystallographic Data Centre, 12 Union Road, Cambridge CB2 1EZ, UK; fax: (+44) 1223-336-033; or deposit@ccdc.cam.uk).

Acknowledgements

We thank Dr. Kunihisa Sugimoto, Rigaku Corporation, for help with the X-ray experiment. We are grateful to Prof. F. Sanda of Kyoto University for the elemental analyses. This work was financially supported by Grant-in-Aid for Research on Basic Area (B-2) No. 12440181 and Scientific Research on Priority Areas (A), No. 413/14045262 from the Ministry of Education, Science, Sports and Culture of the Japanese Government.

[1] J.-M. Lehn, *Supramolecular Chemistry*, VCH, Weinheim, **1995**.
[2] S. J. Rowan, S. J. Cantrill, G. R. L. Cousins, J. K. M. Sanders, J. F. Stoddart, *Angew. Chem.* **2002**, *114*, 938–993; *Angew. Chem. Int. Ed.* **2002**, *41*, 898–952.
[3] a) D. B. Amabilino, J. F. Stoddart, *Chem. Rev.* **1995**, *95*, 2725–2828; b) R. Jäger, F. Vögtle, *Angew. Chem.* **1997**, *109*, 966–980; *Angew. Chem. Int. Ed. Engl.* **1997**, *36*, 930–944; c) G. A. Breault, C. A. Hunter, P. C. Meyers, *Tetrahedron* **1999**, *55*, 5265–5293; d) *Moleuclar Catenanes, Rotaxanes and Knots* (Eds.: J.-P. Sauvage, C. O. Dietrich-Buchecker), Wiley-VCH, Weinheim, **1999**; e) T. J. Hubin, D. H. Busch, *Coord. Chem. Rev.* **2000**, *200–202*, 5–52.
[4] a) I. T. Harrison, *J. Chem. Soc. Chem. Commun.* **1972**, 231–232; b) I. T. Harrison, *J. Chem. Soc. Perkin Trans. 1* **1974**, 301–304.
[5] G. Schill, W. Beckmann, N. Schweickert, H. Fritz, *Chem. Ber.* **1986**, 2674–2655.
[6] a) D. G. Hamilton, N. Feeder, S. J. Teat, J. K. M. Sanders, *New J. Chem.* **1998**, 1019–1021; b) D. G. Hamilton, J. E. Davies, L. Prodi, J. K. M. Sanders, *Chem. Eur. J.* **1998**, *4*, 608–620; c) D. G. Hamilton, M. Montali, L. Prodi, M. Fontani, P. Zanello, J. K. M. Sanders, *Chem. Eur. J.* **2000**, *6*, 608–617.
[7] T. J. Kidd, D. A. Leigh, A. J. Wilson, *J. Am. Chem. Soc.* **1999**, *121*, 1599–1600.
[8] a) S. J. Cantrill, S. J. Rowan, J. F. Stoddart, *Org. Lett.* **1999**, *1*, 1363–1366; b) S. J. Rowan, J. F. Stoddart, *Org. Lett.* **1999**, *1*, 1913–1916; c) P. T. Glink, A. I. Oliva, J. F. Stoddart, A. J. P. White, D. J. Williams, *Angew. Chem.* **2001**, *113*, 1922–1927; *Angew. Chem. Int. Ed. Engl.* **2001**, *40*, 1870–1875.
[9] W. J. Lee, G. M. Whitesides, *J. Org. Chem.* **1993**, *58*, 642–647.
[10] H. Hioki, W. C. Still, *J. Org. Chem.* **1998**, *63*, 904–905.
[11] S.-W. Tam-Chang, J. S. Stehouwer, J. Hao, *J. Org. Chem.* **1998**, *63*, 904–905.
[12] S. Otto, R. L. E. Furlan, J. K. M. Sanders, *J. Am. Chem. Soc.* **2000**, *122*, 12063–12064.
[13] A. G. Kolchinski, N. W. Alcock, R. A. Roesner, D. H. Busch, *Chem. Commun.* **1998**, 1437–1438.
[14] L. Raehm, C. Hamann, J.-M. Kern, J.-P. Sauvage, *Org. Lett.* **2000**, *2*, 1991–1994.
[15] Y. Furusho, T. Hasegawa, A. Tsuboi, N. Kihara, T. Takata, *Chem. Lett.* **2000**, 18–19.

[16] P. R. Ashton, P. J. Campbell, E. J. T. Chrystal, P. T. Glink, S. Menzer, D. Philp, N. Spencer, J. F. Stoddart, P. A. Tasker, D. J. Williams, *Angew. Chem.* **1995**, *107*, 1997–2001; *Angew. Chem. Int. Ed. Engl.* **1995**, *34*, 1865–1869.
[17] N. Watanabe, T. Yagi, N. Kihara, T. Takata, *Chem. Commun.* **2002**, 2720–2721.
[18] B. Beagley, K. T. McAloon, *Trans. Faraday Soc.* **1971**, *67*, 3216–3222.
[19] a) P. R. Ashton, E. J. T. Chrystal, P. T. Glink, S. Menzer, C. Schiavo, N. Spencer, J. F. Stoddart, P. A. Tasker, A. J. P. White, D. J. Williams, *Chem. Eur. J.* **1996**, *2*, 709–728; b) P. T. Glink, C. Schiavo, J. F. Stoddart, D. J. Williams, *Chem. Commun.* **1996**, 1483–1490; c) P. R. Ashton, I. Baxer, M. C. T. Fyfe, F. M. Raymo, N. Spencer, J. F. Stoddart, A. J. P. White, D. J. Williams, *J. Am. Chem. Soc.* **1998**, *120*, 2297–2307.
[20] Y. Marcus, *The Properties of Solvents*, Wiley, Chichester, **1998**.
[21] T. Takata, H. Kawasaki, N. Kihara, Y. Furusho, *Macromolecules* **2001**, *34*, 5449–5456.
[22] Y. Furusho, G. A. Rajkumar, T. Oku, T. Takata, *Tetrahedron* **2002**, *58*, 6609–6613.
[23] *Organic Chemistry of Sulfur* (Eds.: L. Field, S. Oae), Plenum Press, New York, **1977**.
[24] HMPT reacts with **1a** to form the corresponding thiophosphonium salt and thiol **7a**. T. Oku, Y. Furusho, T. Takata, unpublished results.
[25] T. Oku, Y. Furusho, T. Takata, *J. Polym. Sci. Part A: Polym. Chem.* **2003**, *41*, 119–123.

Received: December 5, 2002 [F4644]

